Available online at www.sciencedirect.com

SciVerse ScienceDirect

Energy Procedia 18 (2012) 317 – 326

Energy Procedia

Effect of gas flow velocity in the channels of consumption reactants in a fuel cell type (PEMFC).

M. Zeroual[a], H. Ben Moussa[b], M. Tamerabet[c] a*

[a] *LPEA, Physics Department, faculty of sciences, Batna University, Algeria*
[b] *LPEA, Mechanics Department, Faculty of technology, Batna University, Algeria,*
[c] *LPEA, Mechanics Department, Faculty of technology, Batna University, Algeria,*

.

Abstract

In this work, an isothermal and unsteady three-dimensional model is developed to study the influence of physical and geometric parameters, gas flows in channels, on the consumption of reagents in a fuel cell exchange membrane protons (PEMFC). The equations governing the problem were solved by the finite volume method with a power scheme. The problem of pressure-velocity coupling was solved by the method of projections .. The results show that: the decrease in the rate of gas flow in the channels makes consumption of reagents more uniform. The enlargement of the latter also leads to the same result. The installation of an obstacle, improves consumption of reagents in the case of high speeds.

Key words : fuel cell, PEMFC, hydrogen, channel, reagent, numerical.

1. Introduction:

The technology of fuel cells offers the prospect of producing electricity with zero energy emission. Fuel cells are considered as potential agents sources of energy in the future. One of the important factors that influence the performance of a PEMFC is the configuration of the flow channel in the bipolar plates. The gas flow in the channels has a great influence on the performance of fuel cells proton exchange membrane (PEMFC). Considerable work has been realized to study the influence of the gas flow velocity on the performance of PEMFC. Yan WM et al. [1] use a numerical model to describe the electrochemical processes and transport characteristics of reactive gases and its effect on the performance of PEM fuel cells. The transport of reactants through the electrodes, the length of the canal, the porosity of the gas diffusion layer and the surface of the catalyst layer, have a direct influence on the current density and the

* Corresponding author. Tel.: +213-(0)-33812143; fax: +213-(0)-33812143.
E-mail address: zeroualmos@gmail.com

 doi:10.1016/j.egypro.2012.05.043

resulting transient characteristics of the system. It is found that the increase in current density leads to a faster dynamic response. Ying W et al. [2] developed a mathematical model coupled three-dimensional and validate its results with experimental data. The equations governing the transfer of heat and mass and fluid dynamics are combined with the electrochemical reactions. The numerical solution of the equations is performed using the commercial code STAR-CD based on the methods of the differences and finite volume. The electrochemical characteristics of water transport are also present to study the effect of channel configuration on the overall system performance. Shyam Prasad KB and Jayanti S [3] present a numerical study that describes the passage of gases from one branch to another coil of a channel of a cell PEMFC. A model based on the Navier-Stocks for an incompressible flow, monophasic, and isotherm is developed to study various aspects of the flows related to PEMFC. They determined how water vapor is removed efficiently because of the diffusion and convection in the electrode and the gas channel. Wang XD et al. [4]: A three-dimensional model was used to analyze the effect of design parameters of the bipolar plates (the number of serpentine channels, the number of elbows in each serpentine, and the width of the flow channel) on the functioning a cell PEMFC. The effect of the formation of liquid water in the pores of the porous layers was also considered in the model, while the complex two-phase flow was neglected. The study shows that a flow channel in the form of a simple serpentine, the cell performance improves by increasing the number of bends, as the performance of a single serpentine unit is better than double or triple serpentine. Perng SW et al. [5] present a two-dimensional numerical study on the performance of a fuel cell proton exchange membrane (PEMFC) using the finite element method. Factor studied in this work is the influence of the installation of a chicane in the transverse flow channel on the oxygen consumption and production of the current. The results show that the installation section of a chicane or obstacle in the flow channel can effectively increase the local performance (around the chicane) of a PEMFC. In addition, the effect of an obstacle on the overall performance of the cell is better than a chicane. Perng SW et al. [6] studied numerically the effect of the position and dimensions of a rectangular obstacle, installed in the flow channel on the cathode side, the performance of a cell of a fuel cell proton exchange membrane in using a two-dimensional stationary, isothermal and single phase. The fields of velocity distribution, pressure, and oxygen concentration are presented and analyzed, and the profile of local current density. Shimpalee S et al. [7] present a three-dimensional model that describes the process of transmission, distribution and consumption of reagents and water transport through the membrane. The model makes a change of flow distribution of reactants, which is a more uniform and in a way that reduces the stress distribution. The results show how temperature, water content and distribution of the current density is more uniform field of a serpentine channel with a wider and more roads. You L et al. [8] present a multi-component mathematical model valid in the different components of a cell PEMFC. The model describes the electrical potential, the distribution of current density in the electrodes, and the process of diffusion of gases. The results of this model show the typical distributions of concentrations using a coupling (oxygen-current density). And predicts the various cathodic polarization curves then compared with experimental data. Dewan HA et al. [9] simulated the performance of a cell with inclusion of PEMFC electrodes and for different geometries of the channels under a high electric current density. A three-dimensional model was developed with a straight channel geometry. The simulation results show that a channel of rectangular section gives voltages higher or lower compared to that of trapezoidal or parallelogram, yet the trapezoidal shape facilitates the diffusion of reagents, which leads to a uniform distribution of these and the current density. The simulation of the three geometries, using the same boundary conditions, shows that among the geometric parameters, the width of the ribs is one of the most important parameters, the decrease in the width of the ribs facilitates the distribution of reagents and allows reduce the loss of concentration. Scholta J et al [10] present an experimental study of the influence of channel geometry on the performance of a PEMFC. A parallel channel configuration has been developed. The influence of the channel width and thickness of the ribs on the battery performance was

investigated. An optimum between 0.7 and 1 mm was found for the channel and the width of the ribs. For very small dimensions, the manufacturing very difficult and the probability that the channel becomes blocked by the formation of water droplets increases. In general, the narrow channel dimensions are preferred for high current densities, whereas larger dimensions are better for low current densities. Maher Sadiq Al-Baghdadi MAR [11] develop a model in three dimensions to simulate transport processes for the development and optimization of PEMFC systems. This complete model describes transport phenomena, electrochemical kinetics of the electrodes, the mechanism of phase change and the interaction of many transport phenomena that cannot be studied experimentally. Through this model, species profiles, temperature distribution, voltage and local current density are presented and analyzed for a steady state. Mohammad Akbari MH et al. [12] develop a complete model, a three-dimensional PEMFC. The equations of conservation of mass, momentum, species, energy and charge are solved by finite volume method, taking into account chemical kinetics based on Butler-Volmer equation. In this study the effects of the flow channel dimensions on the operation of the cell are studied. The simulation results indicate that increasing the width of the channel improves the current density. The objective of this work is to achieve a numerical modeling, three-dimensional, transient in order to study the influence of the speed of gas flow in channels, on the consumption of reagents.

2. Mathematical Model

2.1. Computational Domain

The computational domain is limited to a flow channel right. It consists of two gas flow channels cathode and anode, the cathode, the anode and the membrane (fig.1).

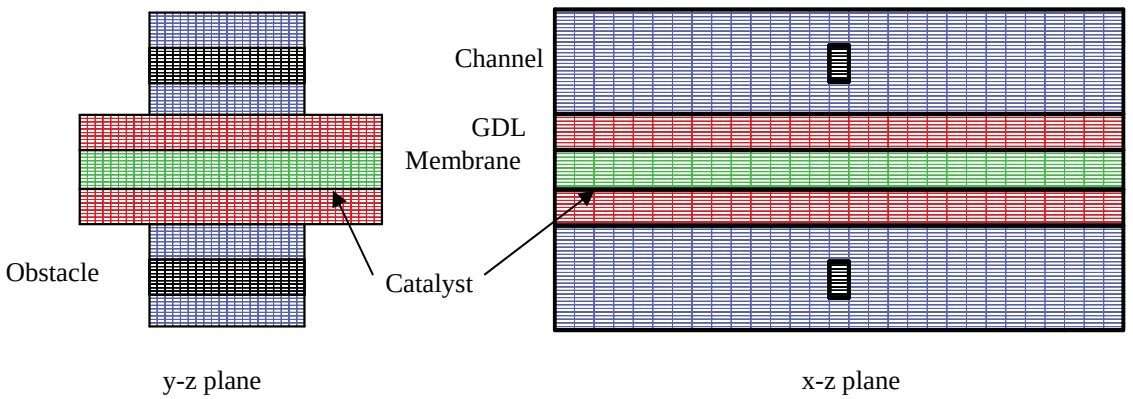

Fig.1. longitudinal and transverse sections of the computational domain.

2.2. Model Assumptions

A complete fuel cell is an extremely complex system involving fluid dynamic, mass transport phenomena and electrochemical reaction feature. In order to achieve a solution of tow-dimensional model of a complete cell it is necessary to do some reasonable simplifying assumptions.
In this model the following assumptions are used:
(1) Flows within channels are considered laminar, incompressible and unsteady;
(2) Water in the flow channels and gas diffusion layers is considered in the vapor phase;
(3) Water is produced as a vapor;
(4) The diffusion layer is homogeneous and isotropic;
(5) The temperature of different parts of the cell is constant;
(6) The membrane is fully humidified so that the ionic conductivity is constant.

2.3. Governing Equations

The dimensionless form the equations governing the problem are:

Continuity equation:

$$\frac{\partial U^*}{\partial x^*} = \frac{\partial V^*}{\partial y^*} = \frac{\partial W}{\partial z^*} = 0 \quad (1)$$

Momentum equations:

$$\frac{\partial U^*}{\partial t^*} + U^*\frac{\partial U^*}{\partial x^*} + V^*\frac{\partial U^*}{\partial y^*} + W^*\frac{\partial U^*}{\partial z^*} = -\frac{\partial P^*}{\partial x^*} + \frac{1}{\varepsilon_d Re}\left(\frac{\partial^2 U^*}{\partial x^{*2}} + \frac{\partial^2 U^*}{\partial y^{*2}} + \frac{\partial^2 U^*}{\partial z^{*2}}\right) - \frac{1}{Re}\frac{\varepsilon_d}{Da_d}U^* \quad (2)$$

$$\frac{\partial V^*}{\partial t^*} + U^*\frac{\partial V^*}{\partial x^*} + V^*\frac{\partial V^*}{\partial y^*} + W^*\frac{\partial V^*}{\partial z^*} = -\frac{\partial P^*}{\partial y^*} + \frac{1}{\varepsilon_d Re}\left(\frac{\partial^2 V^*}{\partial x^{*2}} + \frac{\partial^2 V^*}{\partial y^{*2}} + \frac{\partial^2 V^*}{\partial z^{*2}}\right) - \frac{1}{Re}\frac{\varepsilon_d}{Da_d}V^* \quad (3)$$

$$\frac{\partial W^*}{\partial t^*} + U^*\frac{\partial W^*}{\partial x^*} + V^*\frac{\partial W^*}{\partial y^*} + W^*\frac{\partial W}{\partial z^*} = -\frac{\partial P^*}{\partial z^*} + \frac{1}{\varepsilon_d Re}\left(\frac{\partial^2 W^*}{\partial x^{*2}} + \frac{\partial^2 W^*}{\partial y^{*2}} + \frac{\partial^2 W^*}{\partial z^{*2}}\right) - \frac{1}{Re}\frac{\varepsilon_d}{Da_d}W^* \quad (4)$$

Equation of the quantity of species conservation:

$$\frac{\partial C_k^*}{\partial t^*} + U^*\frac{\partial C_k^*}{\partial x^*} + V^*\frac{\partial C_k^*}{\partial y^*} + W^*\frac{\partial C_k^*}{\partial z^*} = \frac{1}{\varepsilon_d\, Re\, Sc}\left(\frac{\partial^2 C_k^*}{\partial x^{*2}} + \frac{\partial^2 C_k^*}{\partial y^{*2}} + \frac{\partial^2 C_k^*}{\partial z^{*2}}\right) + S_k\frac{h}{C^{ref}} \quad (5)$$

S_k : The source term for the species K.

In the cathodic side, the source terms for oxygen and the production of water are respectively given by:

$$S_{O_2} = -\frac{j}{4F} \quad (6) \qquad ; \qquad S_{H_2O} = \frac{j}{2F} \quad (7)$$

In the anodic side, the source term for hydrogen is given by:

$$S_{H_2} = -\frac{j}{2F} \quad (8)$$

The volume current density j is defined by the Butler-Volmer formula:

$$j = a j_0^{ref}\left(\frac{C_{O_2}}{C_{O_2}^{ref}}\right)\left(e^{\frac{\alpha_c^c F}{RT}\eta_c} - \frac{1}{e^{\frac{\alpha_c^c F}{RT}\eta_c}}\right) \quad (9)$$

Pressure Equation

The resolution of the Navier-Stocks presents a difficulty that lies in the pressure field P is not known because there is no equation that governs this field. The trick numerical we will implement to overcome this difficulty is based on the splitting time step.
The pressure equation is:

$$\frac{\partial^2 P}{\partial x^2}+\frac{\partial^2 P}{\partial y^2}+\frac{\partial^2 P}{\partial z^2}=\left(\frac{\partial\left(-\rho U^{t+\frac{\Delta t}{2}}\right)}{\partial x}+\frac{\partial\left(-\rho V^{t+\frac{\Delta t}{2}}\right)}{\partial y}+\frac{\partial\left(-\rho W^{t+\frac{\Delta t}{2}}\right)}{\partial z}\right)/\Delta t \quad (10)$$

2.4. The initial and boundary conditions

2.4.1. Initial condition

It is assumed that the stack is initially empty (There is no reagent) while the initial concentrations of the different species are zero. The speed was initialized by a null value as:

$$P_0^* = U_0^* = V_0^* = W_0^* = C_{k0}^* = 0 \quad (11)$$

The boundary conditions are applied to all external borders of the computational domain.

2.4.2. Input conditions

The values of velocities, concentrations of species, and the admission pressure at the anode and cathode are imposed (Dirichlet condition).

$$U^* = 1 \quad ; \quad V^* = 0 \quad ; \quad C_{H_2O}^* = 0{,}1 \quad ; \quad P^* = 1 \quad (12)$$

At the cathode, we have: $C_{0_2}^* = 1$; $C_{H_2}^* = 0$ (13)

and in the anode, we have : $C_{0_2}^* = 0$; $C_{H_2}^* = 1$ (14)

2.4.3. Output conditions

At the exit of the flow channels for gas and for all variables, we assume that the gradient in the flow direction (x) is zero (Neumann condition).

$$\frac{\partial U^*}{\partial x^*}=\frac{\partial V^*}{\partial x^*}=\frac{\partial W^*}{\partial x^*}=\frac{\partial P^*}{\partial x^*}=\frac{\partial C_{O_2}^*}{\partial x^*}=\frac{\partial C_{H_2}^*}{\partial x^*}=\frac{\partial C_{H_2O}^*}{\partial x^*}=0 \quad (15)$$

2.4.4. External surfaces

On the external surfaces and in all directions, the boundary conditions for pressure and concentrations of species are of the type Neumann. The speeds on the external surfaces are zero, because of the condition of adhesion to the wall.

$$U^* = V^* = W^* = \frac{\partial P^*}{\partial x^*} = \frac{\partial C_{O_2}^*}{\partial x^*} = \frac{\partial C_{H_2}^*}{\partial x^*} = \frac{\partial C_{H_2O}^*}{\partial x^*} = 0 \quad (16)$$

$$U^* = V^* = W^* = \frac{\partial P^*}{\partial y^*} = \frac{\partial C_{O_2}^*}{\partial y^*} = \frac{\partial C_{H_2}^*}{\partial y^*} = \frac{\partial C_{H_2O}^*}{\partial y^*} = 0 \quad (17)$$

$$U^* = V^* = W^* = \frac{\partial P^*}{\partial z^*} = \frac{\partial C_{O_2}^*}{\partial z^*} = \frac{\partial C_{H_2}^*}{\partial z^*} = \frac{\partial C_{H_2O}^*}{\partial z^*} = 0 \quad (18)$$

2.5. Solution Algorithm

The equations governing the problem were solved by the finite volume method with a power scheme and solved using a computational program. The problem of pressure-velocity coupling was solved by the method of projections. The parameters used for each geometry are shown in the following table:

Table.1. geometric parameters of the cell

parameter	Geometry			
	a	*b*	*c*	*d*
Channel length (mm)	30	30	30	30
Channel width (mm)	1	1	1	1
height of channel (mm)	1	1	1	1
Thickness of the diffusion layer (mm)	1/3	1/3	1/3	1/3
Membrane thickness (mm)	1/3	1/3	1/3	1/3
Width of the ribs (mm)	1/2	1/4	1/2	1/2
Length of the chicane / obstacle (mm)	-	-	3	3
Width of the channel coefficient λ : (λ = Channel width / Width of the ribs)	2	4	2	2

3. Results

3.1. Velocity distribution

The laminar velocity profile is where the highest speed is in the center of the channel, this profile is maintained along the channel. The flow velocity in the GDL is negligible because of the low porosity, so in this area, the mass transfer by diffusion becomes more important than convection.

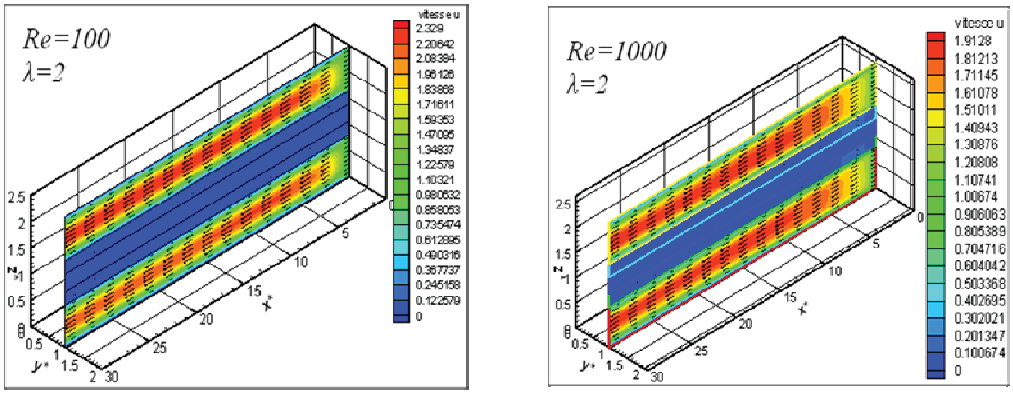

Fig.2: distribution of the velocity field for a single channel.

The installation section of a baffle in the channel, the gas may be required to infiltrate the GDL. The narrowest section of the passage of the channel leads to more gas diffusion layer, but causes a deflection of flow behind the baffle who brings gas from the GDL. The velocity field in the region between the baffle and the catalyst, clearly shows the deviation of the flow to the gas diffusion layer, which means increasing the portion of reactants passing through the area. However, downstream, and because of the deflection, the flow moves and is mainly in the channel and there is little gas in the diffusion layer.

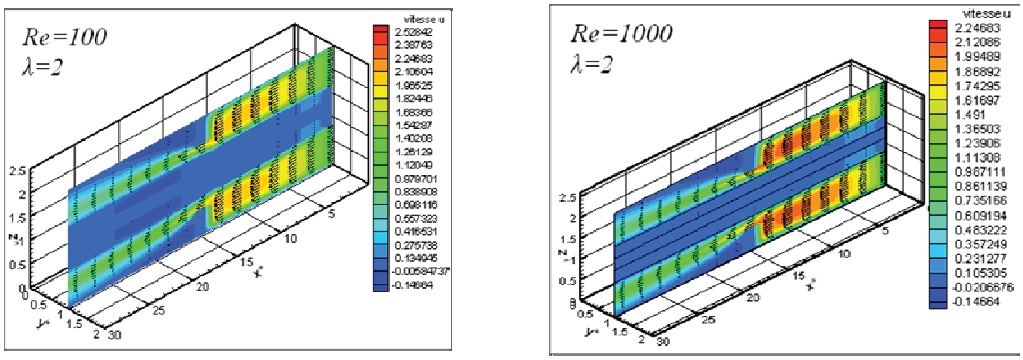

Fig. 3: distribution of the velocity field for a channel with chicane.

The installation of an obstacle, instead of a chicane in the channel may reduce the effect of the deflection by the passage of gas between the collector current and the obstacle. Velocity downstream of the obstacle is lower than upstream because of the loss occurred.

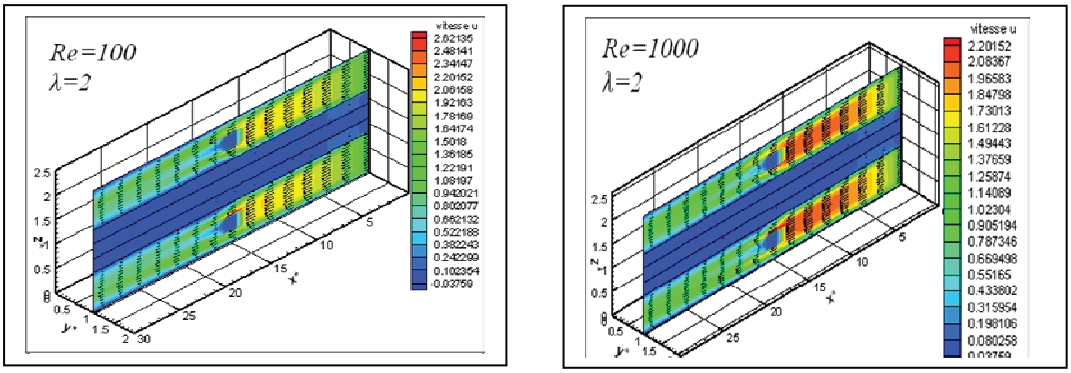

Fig. 4: distribution of the velocity field for a channel with obstacles.

3.2. Hydrogen Distribution

In all cases studied, the hydrogen concentration decreases gradually from the inlet to the outlet of the channel due to consumption of the reactants in the catalyst layer. In the GDL, the concentration of hydrogen in the solid parts (ribs) of the bipolar plate is lower than that in the hollow part (channel). Regarding the distribution of hydrogen concentration in the GDL for simple configuration of the channel, we see that at low Reynolds number, and because of the low consumption rate, more hydrogen is transported by dissemination to the areas under the ribs, leading to a uniform distribution of concentration of this reagent. At a high Reynolds number, the concentration of hydrogen in the veins reaches values close to zero, and since the current density is directly dependent on local concentrations of reagents, the local distribution of current density under the ribs is much less that under the channel. The expansion of channels increases the surface area of the GDL supply of reactant, which increases the rate of consumption.

The effect of installing a chicane in the flow channel on the consumption of reagents was found that the hydrogen consumption generally decreases along the catalyst, but with a peak occurring around the location of the chicane. This peak is caused by the convective force due to the decrease in the flow area which increases the mass transfer.

In order to reduce the effect of the deflection and force more gas to flow into the GDL, the chicane is replaced by an obstacle. Gas flow can be forced to enter the diffusion layer because of the narrow space between it and the obstacle. The effect of deflection, which causes the exhaust of the GDL can be reduced by the passage of gas between the collector current and the obstacle. Downstream of the obstacle in the case of a high Reynolds number, consumption increases because the deflection is just, but less reactive flows through the GDL.

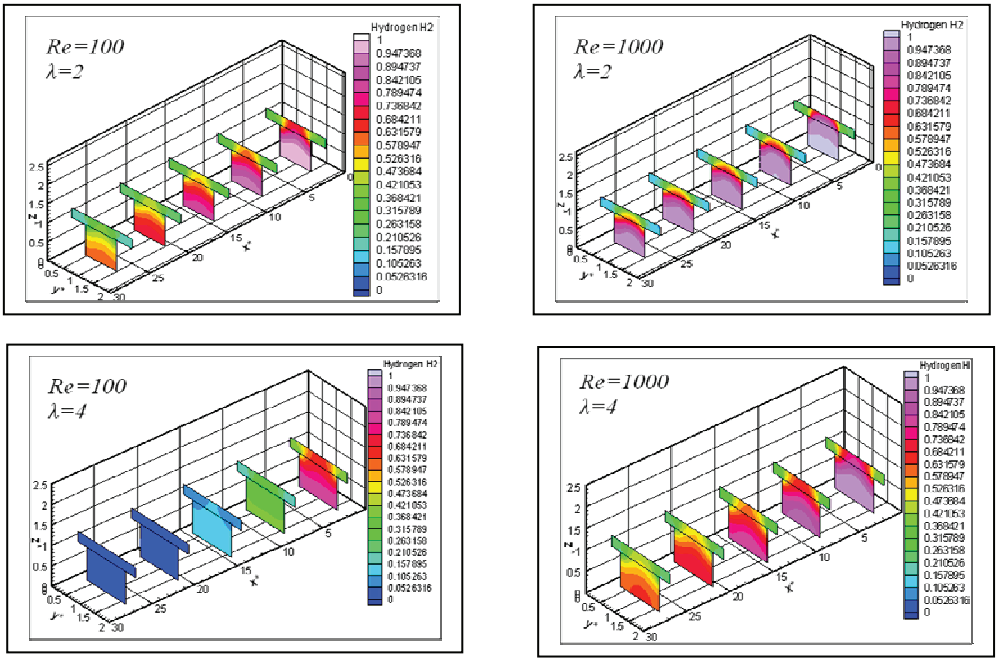

Fig.5: field distribution of hydrogen concentrations for a single channel

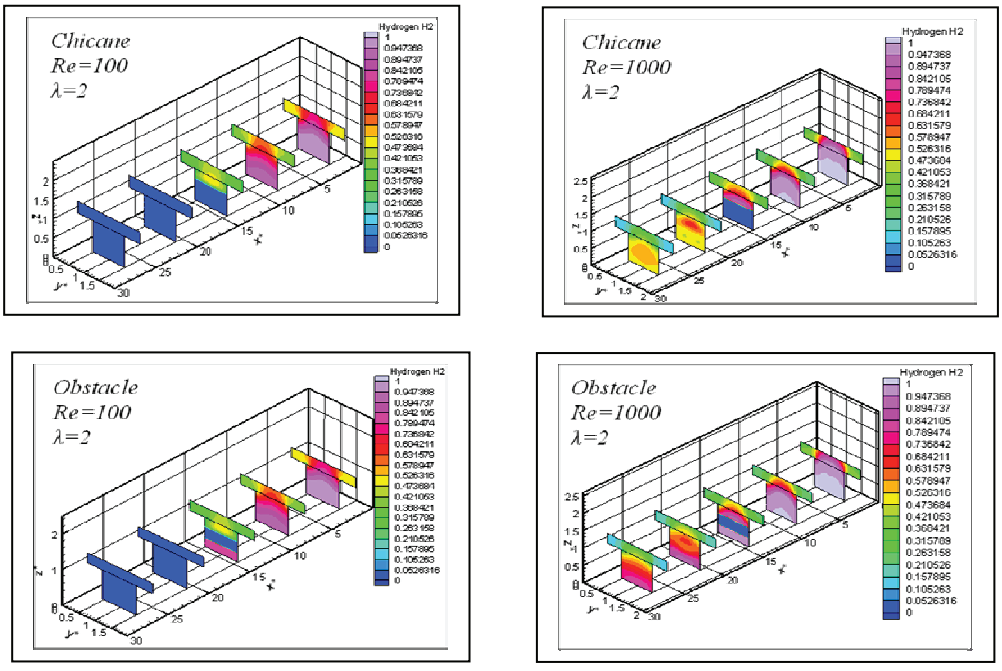

Fig.6: field distribution of hydrogen concentrations

4. Conclusions:

Consumption of reagents becomes more uniform by reducing the rate of gas flow in the channels, which leads to a uniform distribution of current density. A Configuration channel wider and thinner ribs involves more uniform consumption.

The installation of a chicane increases the amount of reagents consumed around her and a resulting increase in current density in this region. Downstream of the chicane, the consumption is very low because of the phenomenon of deflection of the flow which causes the reagents out of the gas diffusion layer.

The replacement of the chicane by an obstacle, in the case of high speeds, reduces the effect of deflection due to the reactive portion of which passes through the gap between the obstacle and the collector current. consumption of reagents increases behind the obstacle, but less reactive flow in the GDL.

The residence time becomes shorter by increasing the speed of gas flow in the channels. The installation of an obstacle in the gas flow channels and the expansion of these reduce the dwell time.

References:

[1] Yan WM, Soong CY, Chen F, Hsin-Sen Chu HS. Transient analysis of reactant gas transport and performance of PEM fuel cells. *Journal of Power Sources* 2005;**143**:48–56.

[2] Ying W, Yang TH, Lee WY, Ke J, Kim CS. Three-dimensional analysis for effect of channel configuration on the performance of a small air-breathing proton exchange membrane fuel cell (PEMFC). *Journal of Power Sources* 2005;**145**:572–581.

[3] Shyam Prasad KB, Jayanti S. Effect of channel-to-channel cross-flow on local flooding in serpentine flow-fields. *Journal of Power Sources* 2008;**180**:227–23.

[4] Wang XD, Duan YY, Yan WM, Peng XF. Local transport phenomena and cell performance of PEM fuel cells with various serpentine flow field designs. *Journal of Power Sources* 2008;**175**:397–407.

[5] Perng SW, Wu HW. Effects of internal flow modification on the cell performance enhancement of a PEM fuel cell. *Journal of Power Sources* 2008;**175**:806–816.

[6] Perng SW, Wu HW, Jue TC, Cheng KC. Numerical predictions of a PEM fuel cell performance enhancement by a rectangular cylinder installed transversely in the flow channel. *Applied Energy* 2009;**86**:1541–1554.

[7] Shimpalee S, Lee Wk, Van Zee JW, Naseri-Neshat H. Predicting the transient response of a serpentine flow- field PEMFC I. Excess to normal fuel and air. *Journal of Power Sources* 2006;**156**:355–368.

[8] You L, Liu H. A two-phase flow and transport model for PEM fuel cells. *Journal of Power Sources* 2006;**155**:219–230.

[9] Dewan HA, Hyung JS. Effects of channel geometrical configuration and shoulder width on PEMFC performance at high current density. *Journal of Power Sources* 2006;**162**:327–339.

[10] Scholta J, Escher G, Zhang W, Kuppers L, Jorissen L, Lehnert W. Investigation on the influence of channel geometries on PEMFC performance. *Journal of Power Sources* 2006;**155**:66–71.

[11] Sadiq Al-Baghdadi MAR. Performance comparison between airflow-channel and ambient air-breathing PEM fuel cells using three-dimensional computational fluid dynamics models. *Renewable Energy* 2009;**34**:1812–1824.

[12] Akbari MH, Rismanchi B. Numerical investigation of flow field configuration and contact resistance for PEM fuel cell performance. *Renewable Energy* 2008; **33**:1775–1783.